Field Tests of 3-Component geophones

Don C. Lawton and Malcolm B. Bertram

ABSTRACT

Field tests of Litton, Geosource and Oyo 3-component geophones showed similar performance characteristics for all three geophones for a test signal generated by a seismic cap at a horizontal distance of 7.5 m from the geophones. Output signal levels from the Litton and Geosource geophones were similar, with the Oyo output being about 20% lower. No cross-coupling between the elements within any of the geophones was observed, but the polarity of all of the horizontal elements is opposite to the recommended SEG standard. There is no consistent colour coding of the clip leads for the various elements between any of the geophones.

Polarization tests for a circle of test shots spaced around the cluster of geophones gave remarkably similar results for all three geophones. Generally, the polarization direction measured by the horizontal elements matched the source azimuth closely, and any deviations were attributed to inhomogeneities in the near-surface sediments.

INTRODUCTION

An important aspect of multicomponent seismic surveys is the performance of the geophones. For example, Stanley (1986) discussed the importance of geophones on data fidelity. There have been several studies which measured the response of geophones in the laboratory (e.g. Hagedoorn, et al., 1988; Krohn, 1984) but there appear to be only a few which deal with geophone performance measured in the field. Krohn (1984, 1985) studied aspects of geophone coupling in laboratory and field experiments for vertical as well as horizontal elements. She showed that the resonant coupling frequency, particularly for horizontal elements, is strongly dependant on geophone coupling, and she emphasised the importance of having the base of the geophone firmly in contact with the ground to ensure that the coupling resonant frequency is above the bandwidth of the reflection data.

This paper describes a field experiment undertaken with three different types of three-component geophones (Oyo, Litton, Geosource). One of each type of geophone was used in the experiment, resulting in 9 channels of data being recorded for each shot. All of the geophones have elements which are arranged in a cartesian configuration, with 2 horizontal elements and one vertical element. According to the suppliers, both the Oyo and Litton geophones have elements with a natural frequency of 10 Hz, whereas the Geosource geophone has a 4 Hz element.

POLARITY

All three geophones have a levelling bubble moulded into the top of the geophone casing, and arrows which show the orientations of the two horizontal elements. In plan view, the Oyo geophone is circular, whereas the Litton and Geosource geophones are both rectangular. Figure 1 shows a photograph of the 3 types of geophones, as deployed in the field for this experiment.

Tap tests with each geophone were performed initially to determine the polarity of each element. For both of the horizontal elements of all three geophones, it was found that
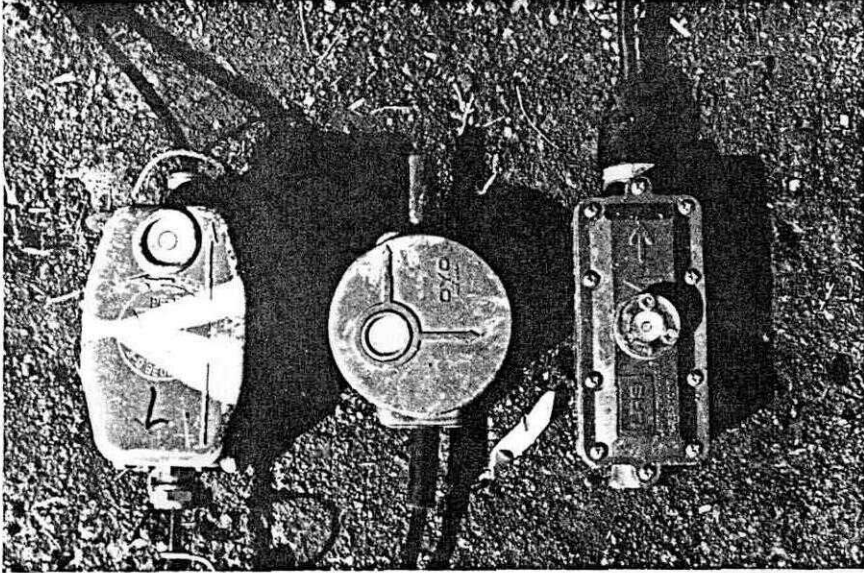
Figure 1. Photograph of the three-component geophones: Geosource (left), Oyo (centre), Litton (right).

Table 1. Colour codes of clip leads.

Geophone	Vertical	Radial	Transverse
Oyo	yellow	red	blue
Litton	red	yellow	black
Geosource	yellow	red	blue
Oyo (rotated)	yellow	blue	red

tapping the geophone case in the direction of the arrow resulted in a trace down-kick; i.e. a negative trace excursion. This is, in fact, opposite to the polarity standard formulated by the S.E.G. for multicomponent geophones Pruett, 1989). On the other hand, the polarity of the vertical component of all geophones is consistent with the S.E.G. polarity standard; i.e. a tap on the top of the geophone case results in an up-kick or positive trace excursion.

TEST PROGRAM

The experiment was undertaken on University of Calgary property at Spy Hill, in northwest Calgary. At the test site, the surface of the ground is flat and the surface layer consists of unconsolidated, poorly sorted glacial till and gravels. The ground surface was cleared and levelled over an area 1 m x 1 m, and the geophones were planted side- by-side in the centre of the cleared area, as shown in Figure 1. The geophones were pressed firmly onto the ground surface to prevent the resonant coupling frequency for the horizontal elements from being too low, caused by geophone 'rocking' (Krohn, 1984).

A reference direction of true north was established and the principal (long) axis of each geophone was oriented in this direction. Since the Oyo geophone is circular, the long axis of this geophone was defined by the position that the clip leads entered the geophone. For this experiment, the element of each geophone which was coaxial with the reference azimuth (0 degrees) was defined as the radial (R) component, and the other horizontal element was defined as the transverse (T) component. In this mode, the positive transverse direction was 270 degrees (west) for the Litton and Geosource geophones, and 90 degrees (east) for the Oyo geophone. Table 1 shows the colour coding for the radial and transverse components of the three geophones, as defined above.

Shotpoints were arranged in a circular pattern around the geophone cluster, as shown schematically in Figure 2. Seismic caps were used as the energy source and the shotpoints were located every 22.5 degrees around the shot circle, giving 16 shotpoints in total. A single cap buried to a depth of 0.25 m was used at each shotpoint. The radius of the shot circle was chosen to be 7.5 m after initial tests showed that this offset did not result in any trace clipping in the instruments. All data were recorded with Sercel 338HR instruments. No low-cut or notch filters were used during data acquisition.

RESULTS

Figure 3 shows a display of the raw data acquired during the experiment, with each group of three traces corresponding to a single shot location. The upper, centre and lower panels in Figure 3 correspond to the vertical, radial and transverse components, respectively, and the source azimuths (Figure 2) are indicated above the panels. No time variant or trace-balance scaling has been applied to the data and, for plotting purposes, the same scalar multiplier was used in each panel. Within each group, the trace order is Oyo, Litton and Geosource consecutively from right to left.

The most obvious feature of the data in Figure 3 is that the outputs from the three geophones are very similar for all three components, except that the Oyo geophone has a slightly lower output (by about 20%) than either of the other two geophones. As expected, the amplitude and phase of the data recorded on horizontal components varies with source azimuth. Generally, the highest amplitudes on these channels were recorded when the source location was in-line with either of the horizontal components.

The waveforms and amplitudes of data recorded by the vertical component (upper panel, Figure 3) show considerable changes as a function of source azimuth, indicating that
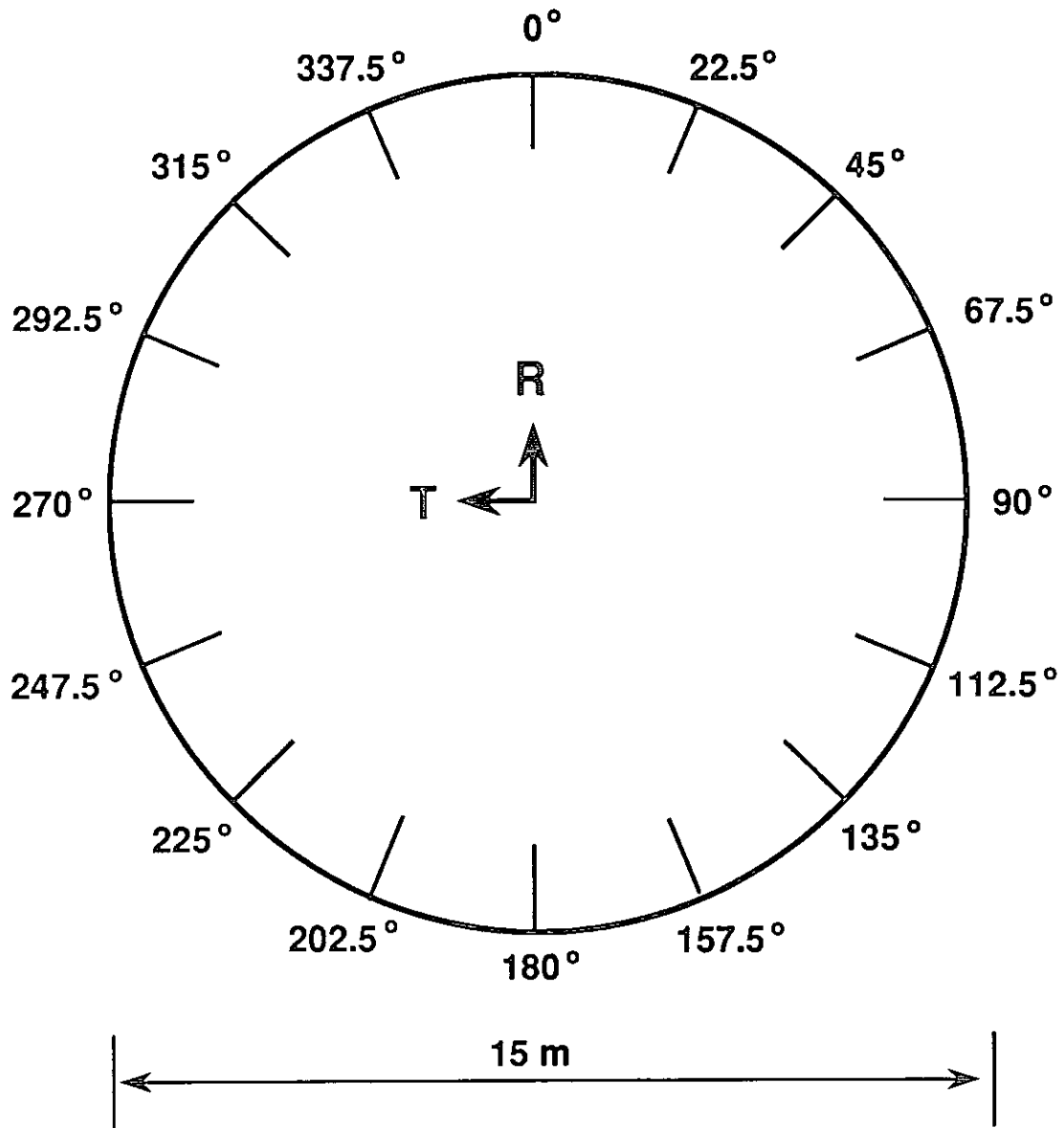
Figure 2. Plan view of shotpoint circle and positive arrow directions of the horizontal elements of the three-component geophones.
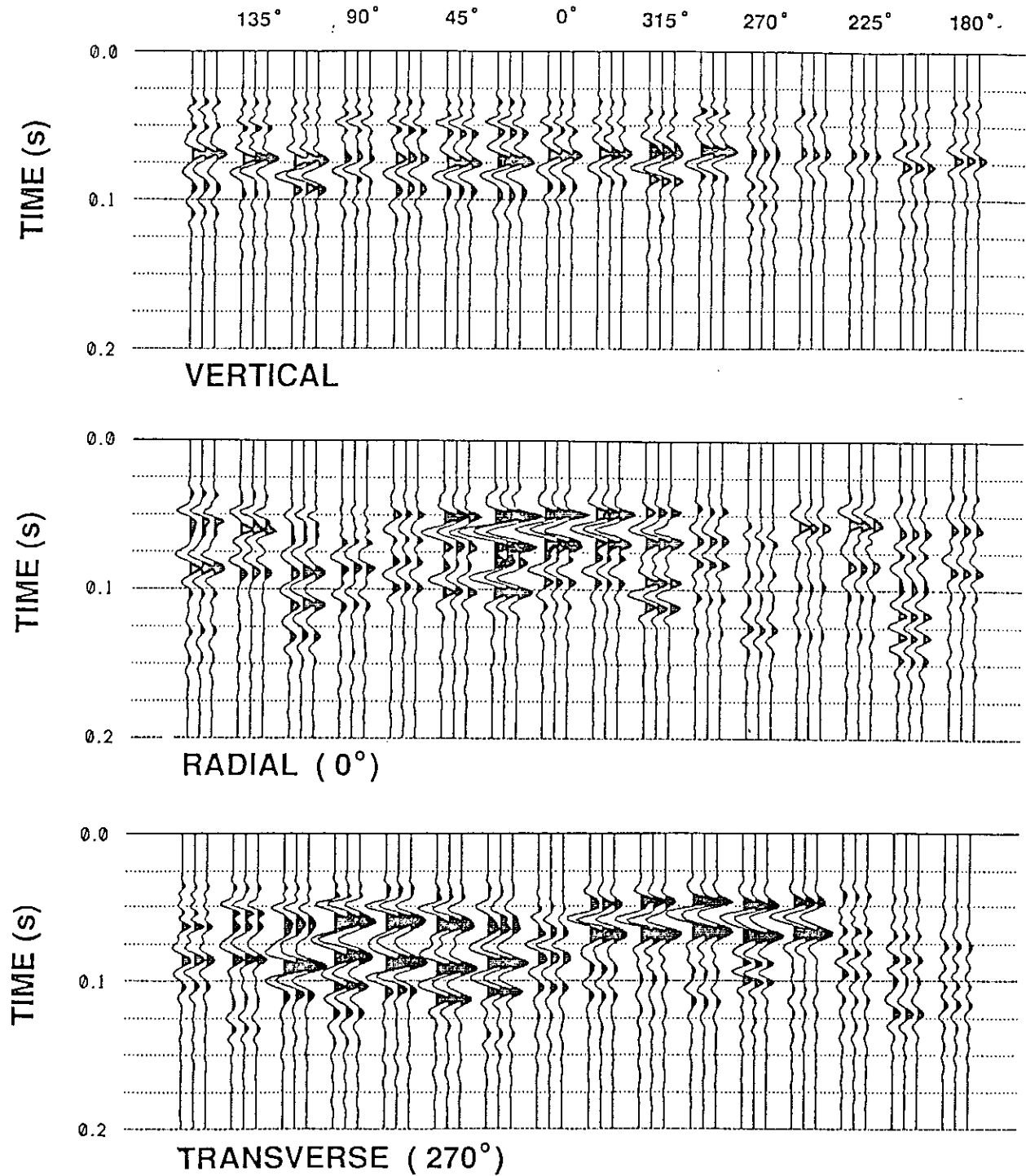
Figure 3. Raw data collected for the source azimuths shown above the top panel; Vertical component (top), radial component (centre) and transverse component (bottom). A scalar multiplier only has been applied.
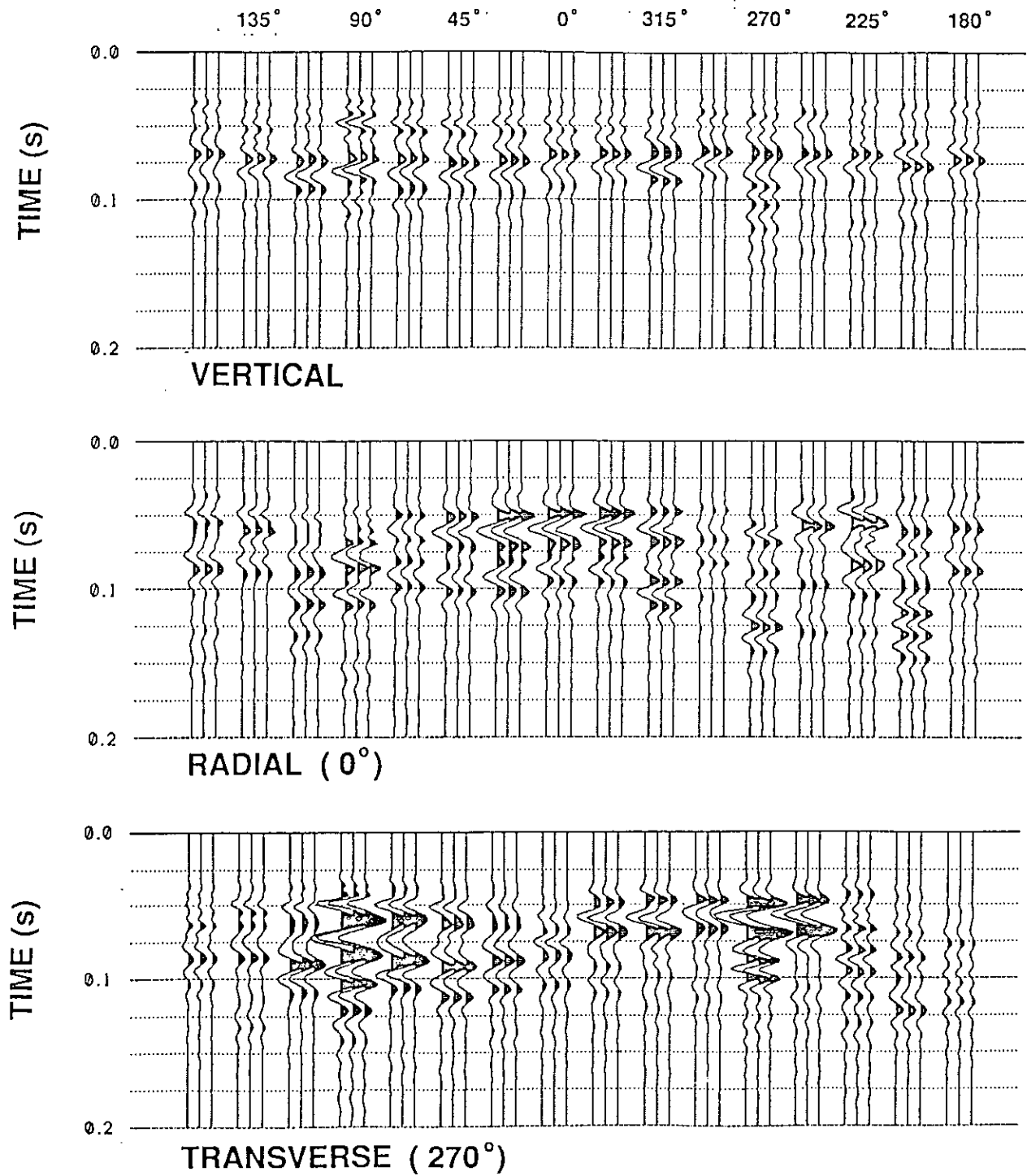
Figure 4. The same data as shown in Figure 3 after amplitude normalization of the vertical component.

the near-surface is inhomogeneous and that the source coupling was not constant. In order to provide an improved visual interpretation of the data, the maximum amplitude of the vertical-component trace was normalised for all shots, and the relevant scaling factor was then applied equally to both of the horizontal components. Data normalised in this manner are shown in Figure 4. The vertical component is now more evenly balanced in terms of amplitude (upper panel, Figure 4), and the horizontal components (centre and lower panels) show more clearly defined amplitude maxima in the principal directions, except for the anomalously low amplitude of the radial component for the source azimuth of 180 degrees. Note that, as expected, the horizontal components show opposite polarity for opposing source azimuths.

Analysis of the data involved hodograms to examine particle motion, and principal axis rotation to examine energy directivity. A prior concern with multicomponent geophones was the possibility of coupling between the three coils within a geophone.
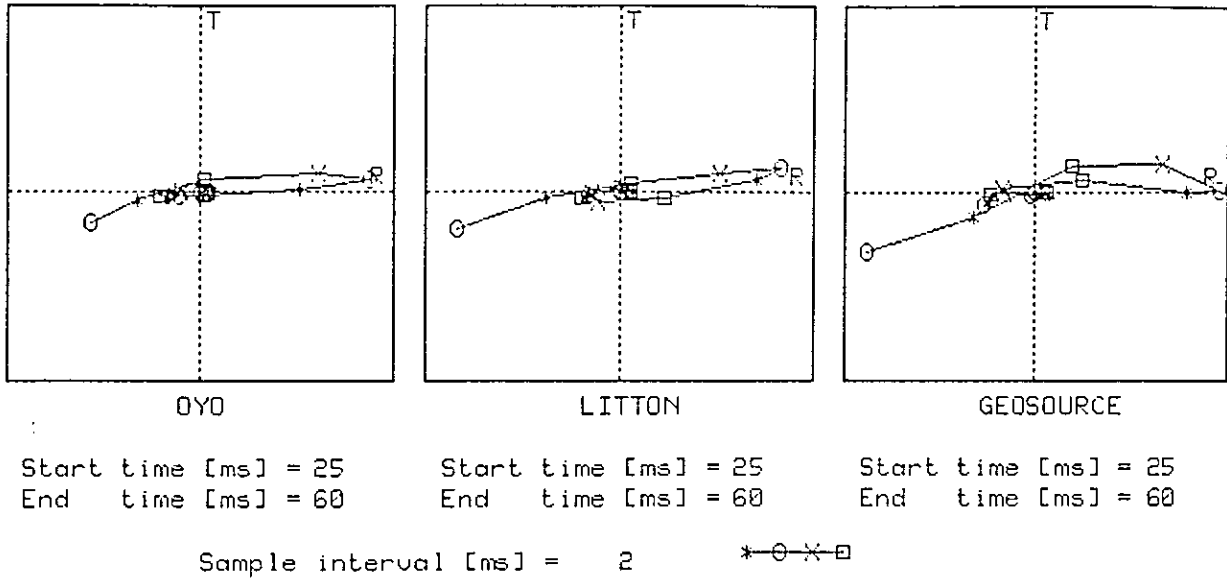
Hodograms of a subset of the entire data volume are presented in Figures 5 to 12. In each hodogram set, the data were scaled to fit the hodogram plotting area so that there is no preservation of relative amplitudes between hodogram sets (i.e. between figures), but the relative amplitudes within each hodogram set are preserved. Figures 5 to 8 show paired hodogram sets for opposing source directions at increments of 45 degrees around the shot circle for a time window from 25 to 60 ms. These hodograms show that the azimuth of particle motion is primarily in the source-receiver direction, with only small particle displacements orthogonal to the source-receiver direction. However, particle motion in the horizontal plane for a source location of 225 degrees (Figure 6) is more complex and is interpreted to be caused by an inhomogeneous weathering layer around this shotpoint. In some of the other hodograms, e.g. at source location 315 degrees (Figure 7), the polarization azimuth of particle motion in the 25 to 60 ms window differs from the source azimuth. However, the deviation from the expected value is similar for all three geophones and is again attributed to near-surface inhomogeneity rather than faulty geophones.

Figure 9 displays hodograms for all components of all three geophones over the time window from 25 to 60 ms, for the shot located at 270 degrees. These hodograms show clearly that the energy arriving at the geophones during this time interval is a horizontally propagating P-wave. This is also shown by the hodograms in the upper part of Figure 10. In the lower part of Figure 10, the particle motion over the time window from 60 to 100 ms is displayed and shows some energy developing on the vertical channel, probably due to a refracted P-wave. However, the complexity of particle motion increases in Figure 11, which shows the superposition of P-waves, Rayleigh waves and Love waves during the time window of 60 to 100 ms for source locations of 0 degrees (Figure 11, upper) and 180 degrees (Figure 11, lower).

Hodograms are a useful technique for displaying particle motion of a vector wavefield and in elucidating wavetypes. Polarization studies were also undertaken by rotating the horizontal coordinate axes in order to maximise the energy on one channel and minimise the energy on the orthogonal channel. This procedure was performed on these data using a method described by DiSiena et al. (1984).

Figure 12 shows a graph of source azimuth versus apparent polarization direction for all 16 shots of the test program. The time window used for the analysis was from 25 to 60 ms, consistent with that used for the hodograms in Figures 5 to 8. Figure 12 thus shows the polarization azimuth at the geophones for the direct P-wave arrival. If the surface layer was perfectly homogeneous, then the polarization angles would equal the source azimuth for all shots; i.e. the data points in Figure 12 would plot along a line with a slope

SOURCE AZIMUTH = 0 DEGREES

OYO   LITTON   GEOSOURCE

Start time [ms] = 25   Start time [ms] = 25   Start time [ms] = 25
End   time [ms] = 60   End   time [ms] = 60   End   time [ms] = 60

Sample interval [ms] =   2   *—O—X—☐

SOURCE AZIMUTH = 180 DEGREES

OYO   LITTON   GEOSOURCE

Start time [ms] = 25   Start time [ms] = 25   Start time [ms] = 25
End   time [ms] = 60   End   time [ms] = 60   End   time [ms] = 60
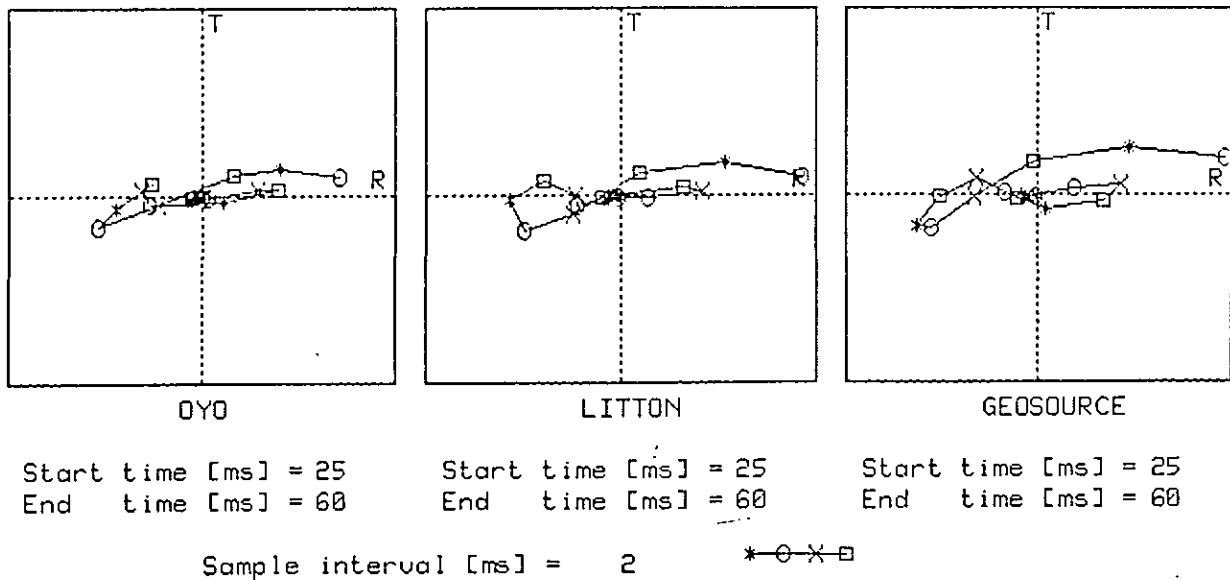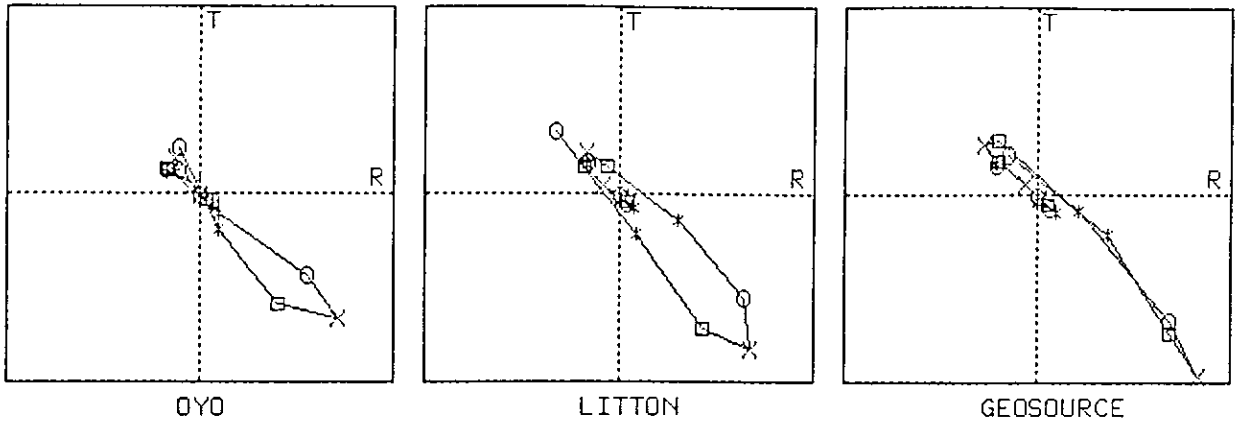
Sample interval [ms] =   2   *—O—X—☐

Figure 5. T-R Hodograms of the direct P-wave arrival for source azimuths of 0 degrees (top) and 180 degrees (bottom).
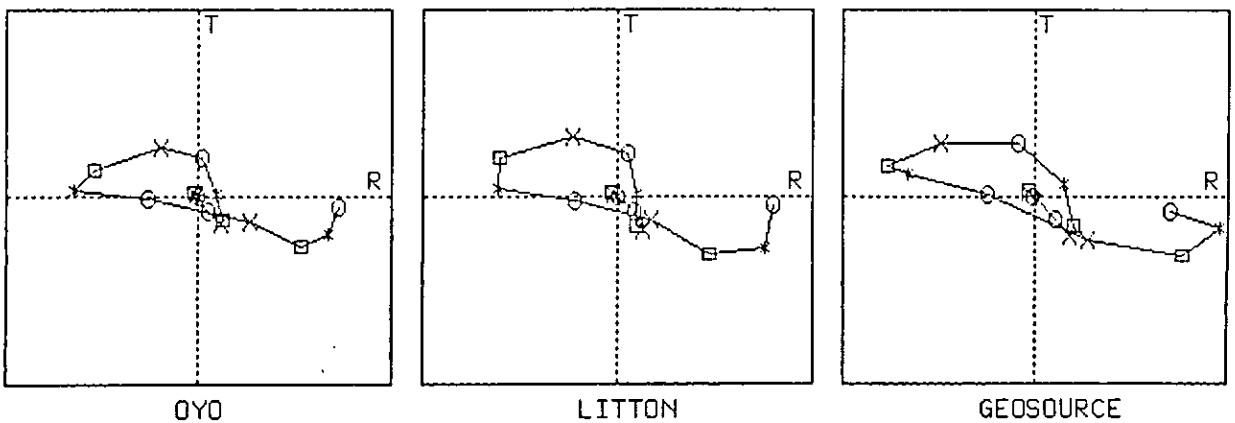
SOURCE AZIMUTH = 45 DEGREES

OYO   LITTON   GEOSOURCE

Start time [ms] = 25
End time [ms] = 60

Start time [ms] = 25
End time [ms] = 60

Start time [ms] = 25
End time [ms] = 60

Sample interval [ms] = 2

SOURCE AZIMUTH = 225 DEGREES

OYO   LITTON   GEOSOURCE

Start time [ms] = 25
End time [ms] = 60
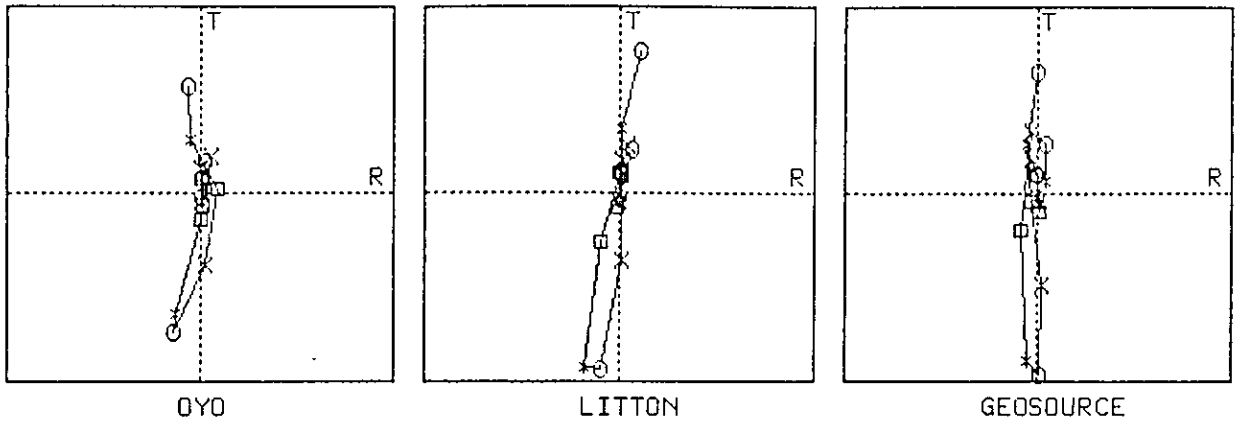
Start time [ms] = 25
End time [ms] = 60

Start time [ms] = 25
End time [ms] = 60

Sample interval [ms] = 2

Figure 6. T-R Hodograms of the direct P-wave arrival for source azimuths of 45 degrees (top) and 225 degrees (bottom).
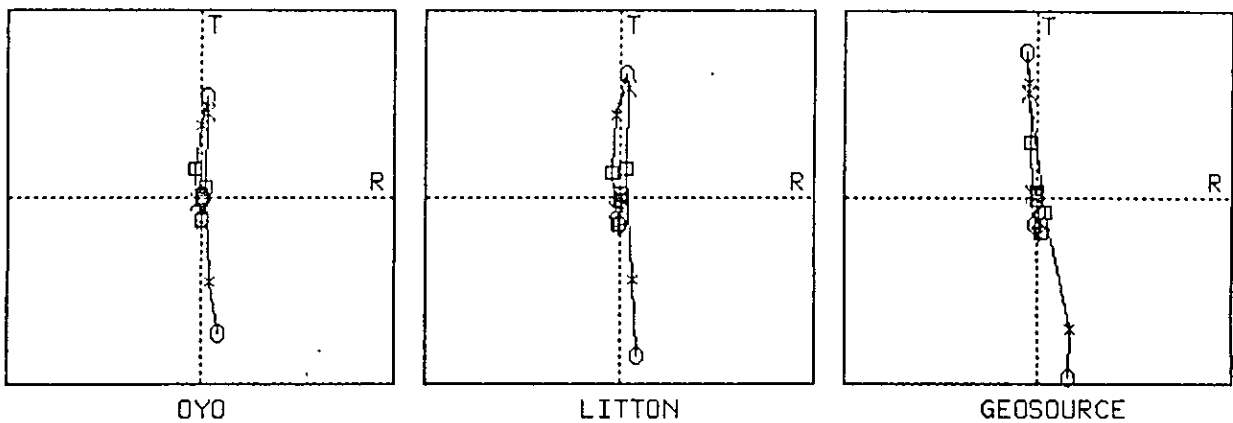
SOURCE AZIMUTH = 90 DEGREES

OYO	LITTON	GEOSOURCE
Start time [ms] = 25	Start time [ms] = 25	Start time [ms] = 25
End time [ms] = 60	End time [ms] = 60	End time [ms] = 60

Sample interval [ms] = 2

SOURCE AZIMUTH = 270 DEGREES

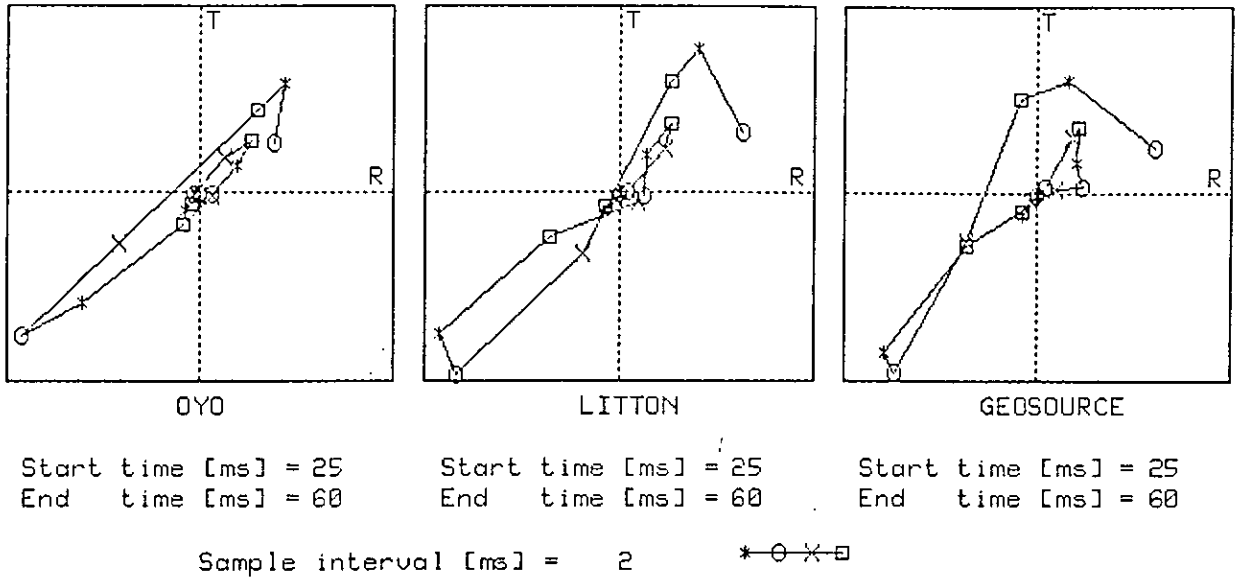|		
OYO	LITTON	GEOSOURCE
Start time [ms] = 25	Start time [ms] = 25	Start time [ms] = 25
End time [ms] = 60	End time [ms] = 60	End time [ms] = 60

Sample interval [ms] = 2

Figure 7. T-R Hodograms of the direct P-wave arrival for source azimuths of 90 degrees (top) and 270 degrees (bottom).

SOURCE AZIMUTH = 135 DEGREES

OYO LITTON GEOSOURCE

Start time [ms] = 25   Start time [ms] = 25   Start time [ms] = 25
End   time [ms] = 60   End   time [ms] = 60   End   time [ms] = 60

Sample interval [ms] =   2   *—O—X—□

SOURCE AZIMUTH = 315 DEGREES

OYO LITTON GEOSOURCE

Start time [ms] = 25   Start time [ms] = 25   Start time [ms] = 25
End   time [ms] = 60   End   time [ms] = 60   End   time [ms] = 60
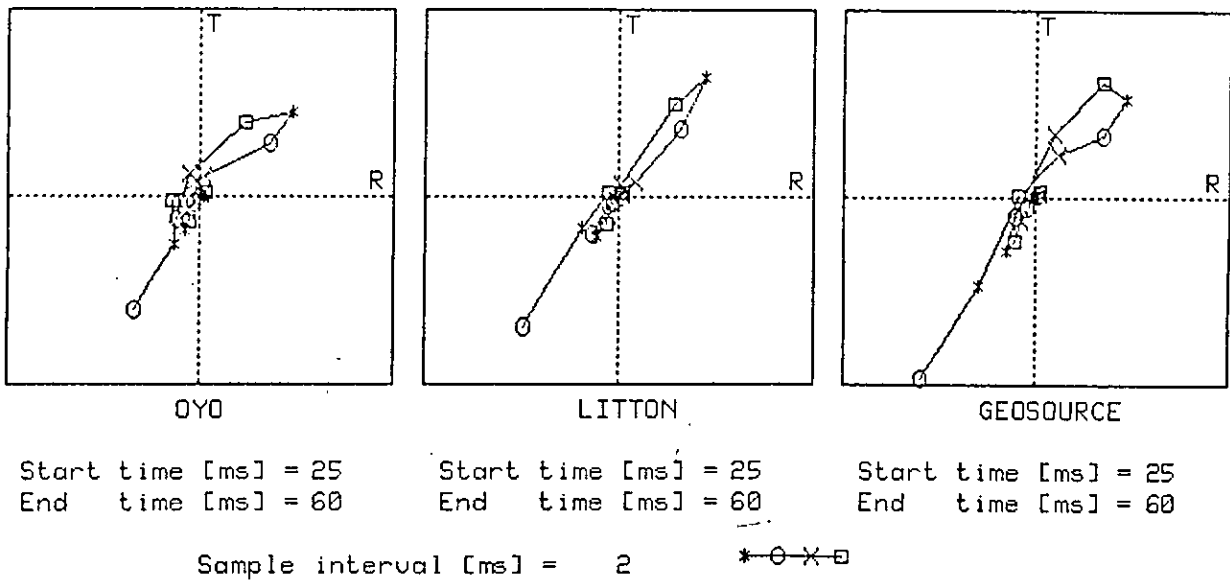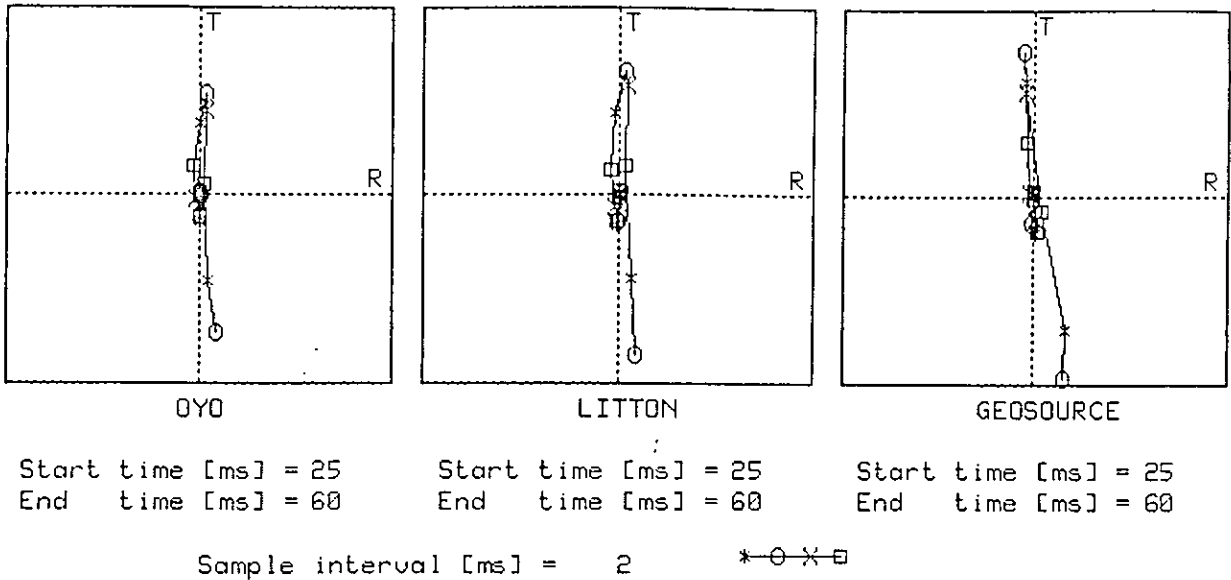
Sample interval [ms] =   2   *—O—X—□

Figure 8. T-R Hodograms of the direct P-wave arrival for source azimuths of 135 degrees
(top) and 315 degrees (bottom).

SOURCE AZIMUTH = 270 DEGREES

| OYD | LITTON | GEOSOURCE |

Start time [ms] = 25   Start time [ms] = 25   Start time [ms] = 25
End   time [ms] = 60   End   time [ms] = 60   End   time [ms] = 60

Sample interval [ms] =   2   *—O—X—☐

SOURCE AZIMUTH = 270 DEGREES

| OYD | LITTON | GEOSOURCE |

Start time [ms] = 25   Start time [ms] = 25   Start time [ms] = 25
End   time [ms] = 60   End   time [ms] = 60   End   time [ms] = 60
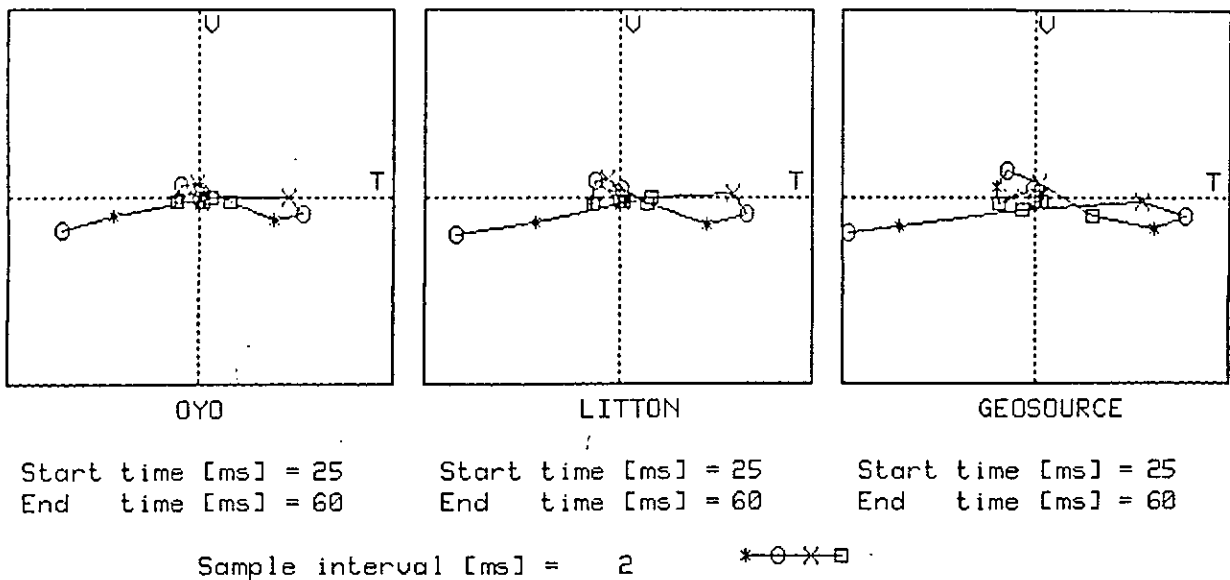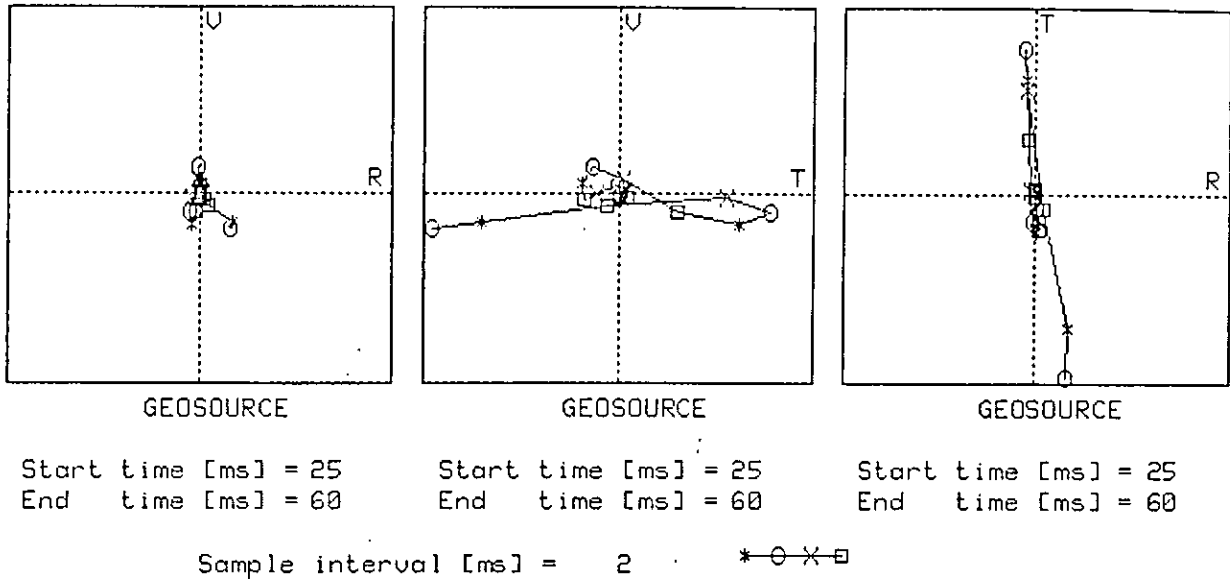
Sample interval [ms] =   2   *—O—X—☐

Figure 9. Hodograms of the direct P-wave arrival for a source azimuth of 270 degrees. T-R components (top) and V-T components (bottom).

SOURCE AZIMUTH = 270 DEGREES

GEOSOURCE   GEOSOURCE   GEOSOURCE

Start time [ms] = 25   Start time [ms] = 25   Start time [ms] = 25
End   time [ms] = 60   End   time [ms] = 60   End   time [ms] = 60

Sample interval [ms] =   2   *—O—X—◻

SOURCE AZIMUTH = 270 DEGREES

GEOSOURCE   GEOSOURCE   GEOSOURCE

Start time [ms] = 60   Start time [ms] = 60   Start time [ms] = 60
End   time [ms] = 100   End   time [ms] = 100   End   time [ms] = 100

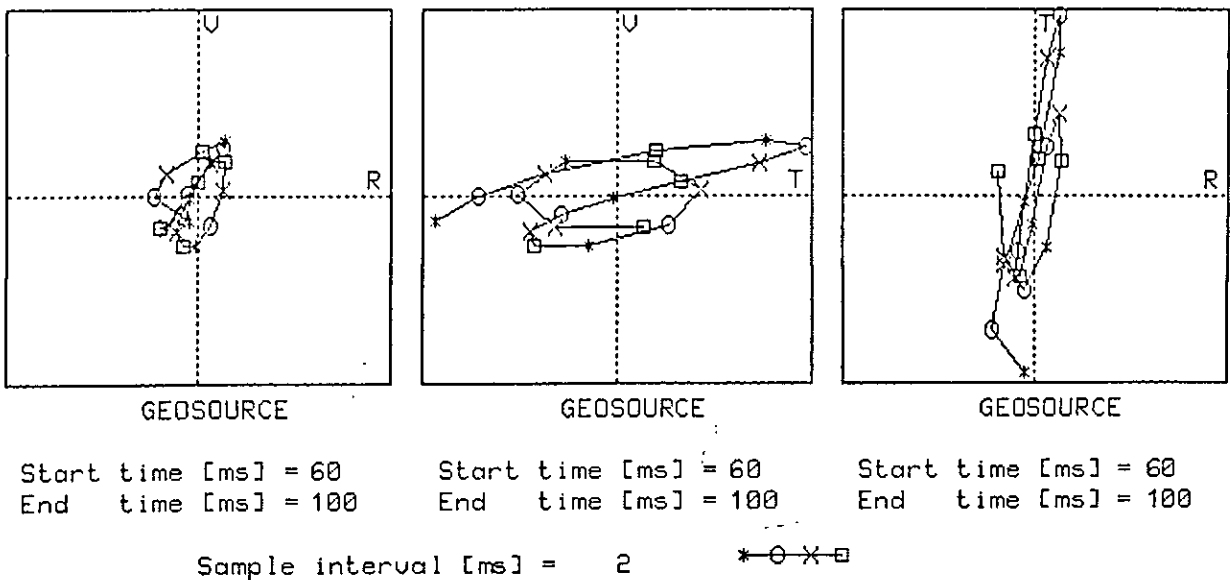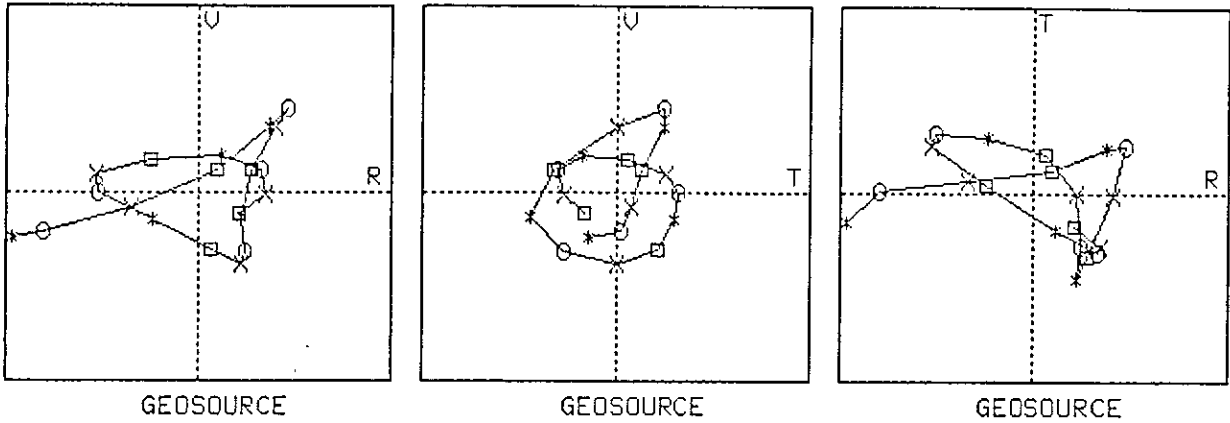Sample interval [ms] =   2   *—O—X—◻

Figure 10. Hodograms for time windows 25 to 60 ms (top) and 60 to 100 ms (bottom), for a source azimuth of 270 degrees and the Geosource geophone. V-R hodograms (left), V-T hodograms (centre) and T-R hodograms (right).
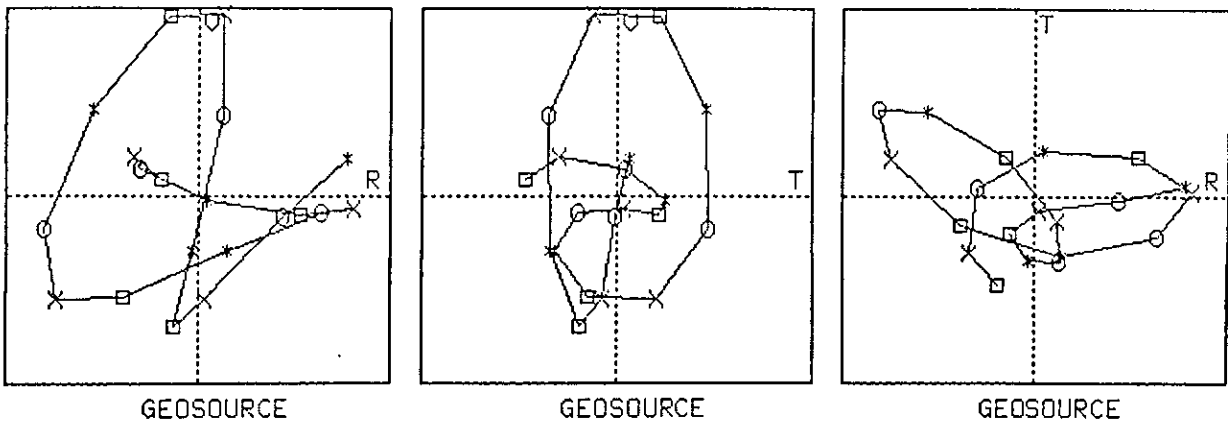
SOURCE AZIMUTH = 0 DEGREES

GEOSOURCE   GEOSOURCE   GEOSOURCE

Start time [ms] = 60   Start time [ms] = 60   Start time [ms] = 60
End   time [ms] = 100   End   time [ms] = 100   End   time [ms] = 100

Sample interval [ms] =   2   *—O—X—◻

SOURCE AZIMUTH = 180 DEGREES

GEOSOURCE   GEOSOURCE   GEOSOURCE

Start time [ms] = 60   Start time [ms] = 60   Start time [ms] = 60
End   time [ms] = 100   End   time [ms] = 100   End   time [ms] = 100

Sample interval [ms] =   2   *—O—X—◻

Figure 11. Hodograms for the time window from 60 to 100 msand source azimuths of 0
degrees (top), 180 degrees (bottom), recorded by the Geosource geophone. V-
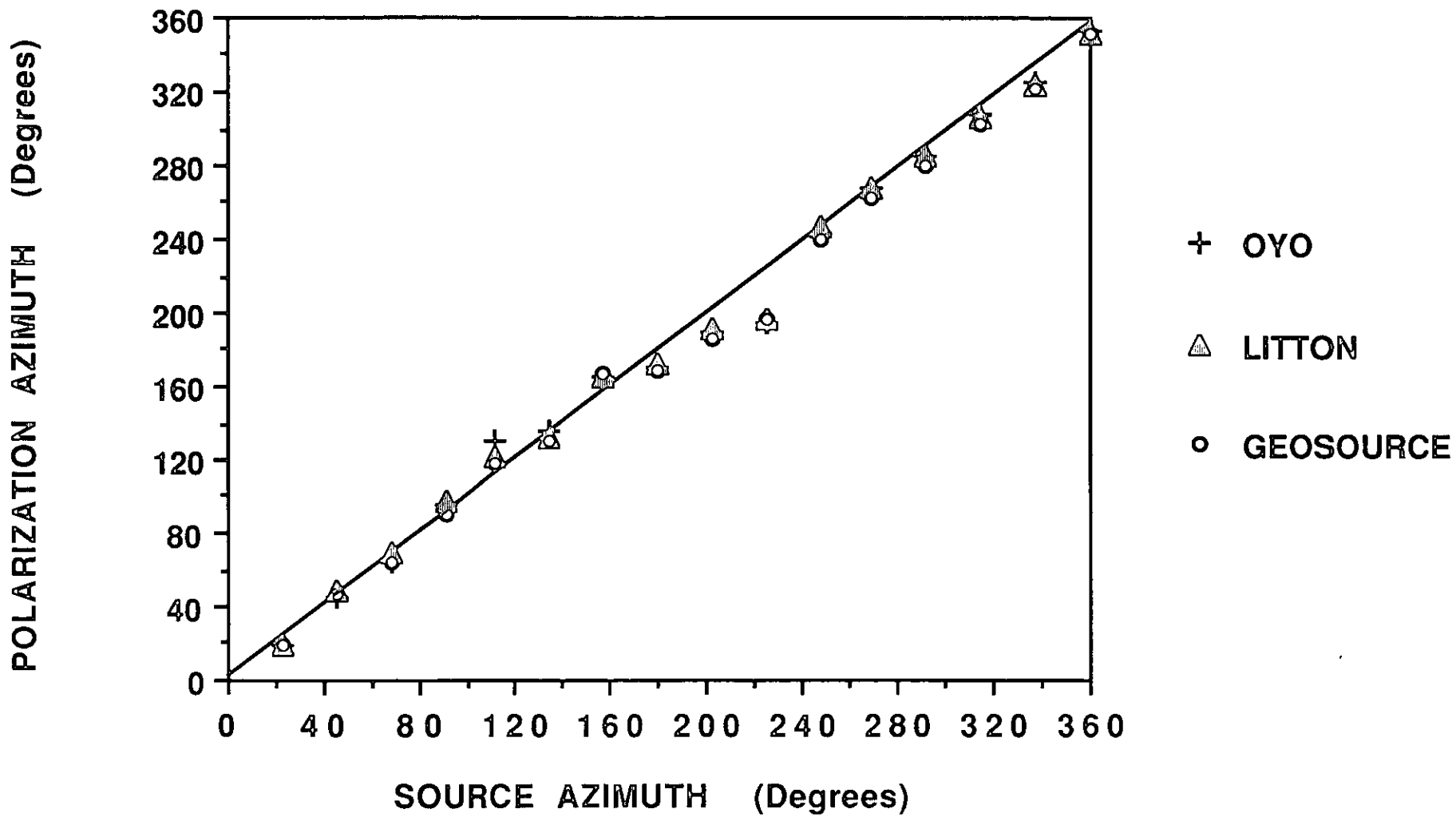R hodograms (left), V-T hodograms (centre) and T-R hodograms (right).

Figure 12. Plot of measured horizontal polarization versus source azimuths for all source locations shown in Figure 2.

of 45 degrees. The actual data show some scatter from the 45 degree line, particularly between source azimuths of 180 to 225 degrees. However, the polarization angles for all three geophones are quite comparable for all shots, so the scatter is interpreted to be caused by near-surface velocity inhomogeneity.

DISCUSSION

The test program has shown that the performance characteristics of the three geophones are very similar and that any one of the three types could be used in a multicomponent seismic survey with equal confidence. However, the bandwidth of the test waveform, generated from a seismic cap at a small offset (7.5 m), was above the natural frequencies of all three of the geophones, and it is recommended that additional tests be undertaken for data containing significant amplitudes of frequencies in the 5 to 10 Hz range.

From a practical standpoint, the Oyo geophone is the easiest to level because it has only 2 spikes (1 long and the other short), whereas the Geosource and Litton geophones have 3 spikes. However, because the Oyo geophone is circular, it is more prone to orientation errors (90 or 180 degrees, typically) than the other two types, which are rectangular. Also, for this test, the 'radial' component of the Oyo geophone was defined to be in the same direction that the geophone leads entered the case (as shown in Figure 1).
In this mode, the positive direction of the 'transverse' component is opposite to that for the Geosource and Litton geophones (Figure 1). After the tests were completed, we realized that if the Oyo geophone was simply rotated 90 degrees counter-clockwise, then the positive directions of the horizontal elements would be the same as the other two geophones. This requires that the location that the geophone leads enter the case be redefined as the 'transverse' direction. While this is quite acceptable, experience from field programs has shown that there is a natural tendency to align the geophone leads in the 'radial' direction.

The lack of consistent colour coding of the geophone leads means that the definition of each component has to established empirically prior to a multicomponent seismic survey. Also, it should be noted that the polarities of the horizontal elements are opposite to the SEG recommendation. For the geophones tested, the horizontal elements of all three types produced a negative voltage when the geophone case was tapped in the direction of the arrow stamped on the case.

CONCLUSIONS

The following conclusions were drawn from the test program:

1. All three geophones tested yielded very similar waveforms for all three components.
2. The signal output levels for the Litton and Geosource geophones were very close to each other, whereas the signal output level from the Oyo geophone was about 20% lower. This applies to all three components.
3. None of the geophones exhibited measureable cross-couplingbetween elements.
4. The polarities of the horizontal elements of all three geophones are equivalent, but are opposite to the recommended SEG standard for multicomponent geophones.
5. There is no consistency in colour coding of the clip leads for the three components between the three geophones tested.
6. Where the near-surface sediments are reasonably homogeneous, the observed polarization azimuths for horizontally propagating P-waves are very close to the source azimuths.

7. Some near-surface velocity inhomogeneity was observed in the shot circle area, between source azimuths of 180 to 225 degrees. The apparent polarization direction measured at these azimuths was consistent for all three geophones.

ACKNOWLEDGEMENTS

REFERENCES

DiSiena, J.P., Gaiser, J.E., and Corrigan, D., 1984, Horizontal components and shear wave analysis of three-component data: in Toksöz, M.N. and Stewart, R.R. Eds.,Vertical seismic profiling, Part B: Advanced concepts: Geophysical Development Series No 14. Geophysical Press.

Hagedoorn, A.L., Kruithof, E.J., and Maxwell, P.W., 1988, A practical set of guidelines for geophone element testing and evaluation: First Break, 6, 325-331.

Krohn, C.E., 1984, Geophone ground coupling: Geophysics, 49, 722-732.

Krohn, C.E., 1985, Geophone ground coupling: Leading Edge, 4, 56-60.

Pruett, R.A., 1989, Polarity documentation for multicompo nent seismic sources and receivers: Abstract, SEG Research Workshop on vector wavefields, Snowbird, Utah, August, 1989.

Stanley, P.J., 1986, The geophone and front-end stability: First Break, 4, 11-14